# Comparison of Soil Samples with Different Clay, Sand, and Silt Contents Using Speckle Interferometry


Felipe Maia Prado
*Center of Lasers and Applications*
*Nuclear and Energy Research Institute*
São Paulo, Brazil
https://orcid.org/0000-0001-9350-2496

Gustavo Di Chiacchio Faulin
*Precision Agriculture*
*Fatec Pompeia*
São Paulo, Brazil
https://orcid.org/0000-0002-8136-322X

Luis Eduardo Rissato Zamariolli
*Soil and Plant Tissue Laboratory*
*Fatec Pompeia*
São Paulo, Brazil
luis.zamariolli01@fatec.sp.gov.br

Pedro Miho de Souza
*Optics and Applications Group*
*Fatec Itaquera*
São Paulo, Brazil
https://orcid.org/0009-0000-7592-3318

Niklaus Ursus Wetter
*Center of Lasers and Applications*
*Nuclear and Energy Research Institute*
São Paulo, Brazil
https://orcid.org/0000-0002-9379-9530

Sidney Leal da Silva
*Optics and Applications Group*
*Fatec Itaquera*
São Paulo, Brazil
https://orcid.org/0000-0001-7663-5545



2025 SBFoton International Optics and Photonics Conference (SBFoton IOPC) | 979-8-3315-9497-8/25/$31.00 ©2025 IEEE | DOI: 10.1109/SBFOTONIOPC66433.2025.11218584



***Abstract*— This study contrasts the Speckle intensity curves of soil samples with clay and sand. The technique used was Speckle interferometry and the analysis was the computational method based on the Time History Speckle Pattern, THSP, and Error Theory.**



***Keywords—Speckle, Soil characterization, THSP***


## I. Introduction

In general, soils with high clay content are dense and compact, with high water and nutrient retention capacity, but they may suffer from poor drainage and aeration. Sandy soils, by contrast, are well-draining and easier to work with, yet they retain less water and nutrients, which can reduce productivity if not managed carefully. Silty soils on the other hand retain more nutrients than sand while being more workable than clay. Understanding the proportions of these components helps inform irrigation planning, fertilizer application, and crop selection, all key aspects of sustainable and efficient agricultural productivity [1,2].

In Brazil, soil texture classification is primarily carried out using standardized gravimetric methods described by the *Empresa Brasileira de Pesquisa Agropecuária* (EMBRAPA) [3]. These techniques mainly rely on the sedimentation behavior of soil particles in water and require the dispersion of the sample, followed by long periods of decantation to separate sand, silt, and clay fractions [3,4] While reliable, these methods are labor-intensive, time-consuming, and depend on controlled laboratory conditions. As a result, they are often impractical for high-throughput analysis or field-based assessments, especially when large areas or real-time decisions are involved.

Given the limitations of conventional methods, there is increasing interest in the development of faster, non-invasive, and automated approaches to soil texture characterization. Optical methods can offer promising alternatives due to their sensitivity to microstructural and compositional differences in materials.

Techniques such as reflectance spectroscopy [5], laser diffraction analyses [4], and speckle analysis [6] have shown potential for capturing texture-related information in soils without altering the sample or needing a long analysis time. Among these, speckle interferometry stands out as a cost-effective and highly sensitive optical method capable of detecting surface and internal differences in soil without disturbing the sample, enabling field-based measurements.

By analyzing the static or dynamic behavior of interference patterns produced under coherent illumination [7,8], speckle interferometry has been used in non-destructive testing, weld quality assessment, and even biomedical evaluations [9-11]. Dynamic laser speckle has been used to estimate the specific surface area of natural and modified bentonite, showing agreement with standard physicochemical assessments [13]. More recently, speckle interferometry with THSP-inspired analysis has been reported to differentiate soil samples by clay content, indicating feasibility for textural discrimination [6].

In this work, we present a speckle-based quantitative approach to assess the clay content in soil samples, particularly contrasting samples with different proportions of clay and sand. The method combines reflection-mode speckle interferometry with computational analysis based on the Time History Speckle Pattern (THSP) [13] and Error Theory [14], providing a reliable and efficient technique for soil contrast analysis.

## II. Theory

The speckle interferometry technique used in this study involves recording videos of speckle patterns generated by coherent light reflected from soil samples. Each frame of the video captures a distinct speckle pattern, and these sequential frames are used to construct a THSP image, which maps the temporal evolution of pixel intensities. The resulting THSP enables the computation of normalized average intensity values as a function of time, reflecting microstructural variations on the soil surface associated with differences in soil content.

Each THSP file is represented as a matrix that has n (rows) x m (columns) that are associated with light intensities (I). The relative average intensity, $\langle I \rangle_j$ (j = 1, 2, …, m), is determined by expression (1):

$$\langle I \rangle_j = \frac{1}{n} \sum_{i=1}^{n} \frac{I_i}{I_{max}} \quad (1)$$


Fundação de Amparo à Pesquisa do Estado de São Paulo (2022/15276-0, 2012/18162-4, 2019/23700-4). Faculdade de Tecnologia de Pompeia (Fatec Pompeia) and Faculdade de Tecnologia de Itaquera (Fatec Itaquera).

where $\langle I\rangle_j$ is the mean intensity over the pixels in the j-frame, and $I_{max}$ is the maximum intensity value across all pixels and frames of the sequence.

Figure 1 presents a diagram of the THSP file generation. Where each column corresponds to the intensity profile of a single pixel line at a given time, while the horizontal axis represents the progression of time.

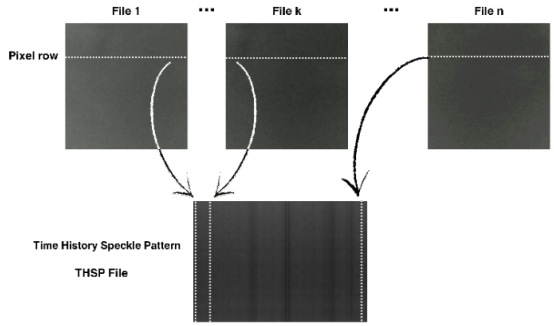


Fig. 1. Construction of the THSP file. A horizontal pixel line (dashed white line) is extracted from each speckle image acquired sequentially. These lines are stacked side-by-side in temporal order to form a 2D image (bottom), resulting in the THSP file. Files k and n represent arbitrary speckle frames acquired between the first and the last frame in the sequence.

To estimate the uncertainty, $\sigma_{\langle I\rangle_j}$, each $\langle I\rangle_j$, we assume Gaussian error propagation [14] and use equation (2).

$$\sigma_{\langle I\rangle_j} = \pm\sqrt{\frac{1}{n\,(n-1)}\sum_{i=1}^{n}(I_i - \langle I\rangle_i)^2} \qquad (2)$$

For a correct contrast comparison, we then correct the intensity $\langle I\rangle_j$ to take into account a proportionality factor, $\langle f\rangle_{\pm Clay}$, and an environmental factor, $f_e$. This correction is done to account for different proportional content of materials and environmental conditions during measurement (e.g., temperature, pressure, and humidity).

The final corrected relative intensity, $\langle I\rangle_{j-n}$, is defined with equation (3.a), with its estimated uncertainty being defined in equation (3.b) [14].

$$\langle I\rangle_{j-n} = \langle I\rangle_j \langle f\rangle_{\pm Clay} f_{env.factor} \qquad (3.a)$$

$$\sigma_{\langle I\rangle_{j-n}} = \pm\langle I\rangle_{j-n}\sqrt{\left(\frac{\sigma_{\langle I\rangle_j}}{\langle I\rangle_l}\right)^2 + \left(\frac{\sigma_{\langle f\rangle_{\pm clay}}}{\langle f\rangle_{\pm clay}}\right)^2 + \left(\frac{\sigma_{f_e.}}{f_e.}\right)^2} \qquad (3.b)$$

The clay-correction factor ($\langle f\rangle_{\pm clay}$) was estimated from reference of each one of the samples with known clay fractions. The environmental factor ($f_{env.factor}$) was derived from the temperature, pressure, and humidity recorded during each acquisition. For each condition we recorded approximately 10 THSP sequences, each comprising about 2,000 frames. The THSP intensity metric (Eq. 1) was computed per sequence as the mean across frames.

## III. Methodology

### A. Soil Samples

The work carried out used soil samples with higher and lower percentages of clay, identified by codes 111214/9 and 106489/4, respectively, as shown in the photos in Figure 2.

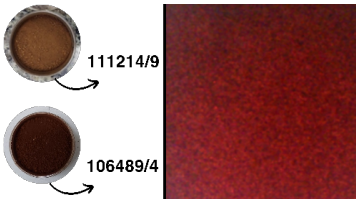


Fig. 2. Soil samples: more clayey (111214/9), less clayey (106489/4), and a speckle pattern image on the right.

### B. Experimental Setup

For the intensity measurements, a reflective speckle interferometer was employed. The experimental setup began with a He-Ne laser emitting at 632 nm, followed by a spatial filter consisting of an objective lens and a 30 µm pinhole. A plan-convex lens was used to collimate the light, and an iris was used to control the diameter of the light beam. Two linear polarizers (Pol. 1 and Pol. 2) were used for contrast adjustment and intensity control. A plane mirror was used to redirect the light onto the soil sample. The speckle pattern generated by the reflected light was recorded as a video using a camera. Figure 3 presents a scheme of the experimental setup.

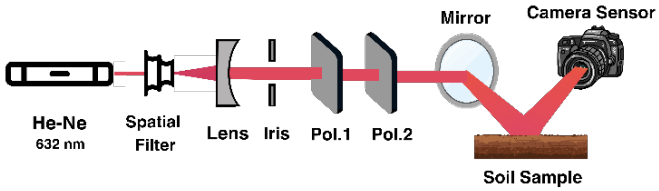


Fig. 3. Speckle experimental setup: Speckle reflection interferometer with linear polarizers. He-Ne Laser light; Spatial filter (objective lens and a pinhole); Plan-convex lens; Iris; Linear polarizers (Pol. 1 and Pol. 2); Plane mirror; Digital camera.

The objective of this work is to show quantitative results, taking account error propagation and correction factors, from the computational calculation of relative average intensities using THSP.

## IV. Results

The proportions of Clay, Sand, and Silt for these samples are shown in Table 1.

TABLE I. Proportions of Clay, Sand, and Silt in Soil Samples Used in Data Collection.

| Samples | Sand (g kg$^{-1}$) | Silt (g kg$^{-1}$) | Clay (g kg$^{-1}$) | USDA(*) Soil Texture Classification |
|---|---|---|---|---|
| 106489/4 | 938.0 ± 0.5 | 6.0 ± 0.5 | 56.0 ± 0.5 | Sand |
| 111214/9 | 576.0 ± 0.5 | 178.0 ± 0.5 | 246.0 ± 0.5 | Sand Loam |

(*) United States Department of Agriculture.

TABLE II. Relative Factors of Proportionality of the Amount of Clay in Comparison to Sand.

| Sample | Proportionality factors ($f_p$) |
|---|---|
| **106489/4 (less clayey)** | 0.0597 ± 0.0005 |
| **111214/9 (more clayey)** | 0.4270 ± 0.0009 |

The proportionality factors for clay in relation to sand were calculated based on data from samples 106489/4 (with lower clay content) and 111214/9 (with higher clay content).

Table 2 presents these values, along with their respective uncertainties.

The average values and uncertainties of the environmental conditions, temperature, pressure, and humidity are shown in Table 3.

TABLE III. PROPORTIONALITIES FOR THE ENVIRONMENTAL CONDITIONS OF THE THREE DATA COLLECTIONS.

| Greatness for environmental factors | Collection A (Static) | Collection A (Slow dynamics) | Collection A (Fast dynamics) |
|---|---|---|---|
| Average temperature (<T>) (ºC) | 14.7 ± 0.3 | 19.0 ± 0.3 | 21.2 ± 0.3 |
| Average pressure (<P>) (hPa) | 983 ± 10 | 1027 ± 11 | 1008 ± 12 |
| Average relative humidity (<U>) (%) | 63 ± 6 | 73 ± 6 | 54 ± 6 |

Figure 4 shows the relative average intensity over time for both samples, where the soil with higher clay content (111214/9) exhibits significantly higher relative intensity values compared to the soil with lower clay content (106489/4).

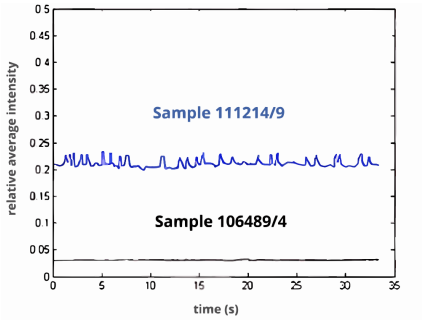


Fig. 4. Distributions of normalized mean relative intensities versus observation times of Speckle interferences from the A1 videos of collection (static) for samples with more (in blue) and less (in black) proportion of clay. The blue and black lines are guides to indicate distribution swings visually.

This difference in average intensity can be attributed to the increased surface roughness and scattering capability of the clay-rich soil, which produces more pronounced and dynamic speckle patterns. The larger fluctuations observed in the 111214/9 sample suggest a greater sensitivity and dynamic behavior, while the signal from the 106489/4 sample remains more stable and lower.

It is important to recognize that soil characterization encompasses a broad spectrum of parameters beyond just the proportions of clay, sand, and silt. Properties such as organic matter content, cation exchange capacity, pH, structure, biological activity, and mineralogy also play crucial roles in soil functionality and agricultural performance. By focusing this study solely on speckle intensity measurements, the results indicate that speckle interferometry can effectively capture relevant contrasts and differences between soil samples with varying clay content, supporting its potential as a complementary tool for soil characterization.

## V. CONCLUSION

The measurements showed higher average relative intensity values for samples with higher clay content (111214/9) compared to those with lower clay content (106489/4). This indicates that differences in clay concentration can be effectively identified through speckle pattern analysis. The methodology proved to be efficient, offering a viable alternative for studying soil texture contrasts.

In future work, the goal is to classify the relative percentages of clay, silt, and sand across various samples to construct a soil contrast map. Additionally, efforts will be made to correct for differences in light absorption among the samples and to further investigate the scattering and dispersion phenomena associated with soils of varying composition.

## REFERENCES

[1] L. N. Centeno, M. D. F. Guevara, S. T. Cecconello, R. O. D. Sousa, and L. C. Timm, “Textura do solo: conceitos e aplicações em solos arenosos,” Rev. Bras. Eng. E Sustentabilidade, vol. 4, no. 1, p. 31, October 2017.

[2] V. A. Klein, M. Baseggio, T. Madalosso, and C. D. Marcolin, “Textura do solo e a estimativa do teor de água no ponto de murcha permanente com psicrômetro,” Ciênc. Rural, vol. 40, no. 7, pp. 1550–1556, July 2010.

[3] Manual de métodos de análise de solos. Embrapa, 2018.

[4] G. S. Faé, F. Montes, E. Bazilevskaya, R. M. Añó, and A. R. Kemanian, “Making Soil Particle Size Analysis by Laser Diffraction Compatible with Standard Soil Texture Determination Methods,” Soil Sci. Soc. Am. J., vol. 83, no. 4, pp. 1244–1252, July 2019.

[5] R. A. Viscarra Rossel, D. J. J. Walvoort, A. B. McBratney, L. J. Janik, and J. O. Skjemstad, “Visible, near infrared, mid infrared or combined diffuse reflectance spectroscopy for simultaneous assessment of various soil properties,” Geoderma, vol. 131, no. 1–2, pp. 59–75, March 2006.

[6] S. da Silva, G. Faulin, L. Zamariolli, P. Souza, F. Prado, and N. Wetter, “Differentiation of clay content in soil samples containing clay, silt and sand using the Speckle methodology,” Brazilian Journal of Physics, to be published.

[7] E. Hecht, Óptica. Lisboa: Fundação Calouste Gulbenkian. Serviço de Educação, 1991.

[8] B. E. A. Saleh and M. C. Teich, Fundamentals of Photonics, 1st ed. Wiley, 1991. doi: 10.1002/0471213748.

[9] D. Prazak and M. Ohlidal, “Laser speckle spectral correlation and surface roughness,” in: 12th Czech-Slovak-Polish Optical Conference on Wave and Quantum Aspects of Contemporary Optics, J, Czech Republic, March 2001, pp. 339–346.

[10] F. M. Prado, D. J. Toffoli, and S. L. Da Silva, “Evaluation of the quality of the shielded metal arc welding process using speckle interferometry,” Rev. Bras. Física Tecnológica Apl., vol. 7, no. 1, April 2020.

[11] S. L. Silva, D. J. Toffoli, I. C. De Biaso, A. C. Santos, C. R. Da Silva, and H. T. Araújo, “Determinação de propriedades mecânicas do aço 1010 sob tensão no regime elástico por meio de speckle dinâmico,” Rev. Bras. Física Tecnológica Apl., vol. 4, no. 1, May 2017.

[12] R. D. Mojica-Sepulveda, L. J. Mendoza-Herrera, G. Bertolini, C. I. Cabello, D. B. Soria, and M. Trivi, “Dynamic laser speckle applied to the determination of the specific surface area of clays,” in Proc. Frontiers in Optics / Laser Science (FiO/LS), OSA Technical Digest. Optica Publishing Group, 2018, paper JW4A.140.

[13] R. Arizaga, M. Trivi, and H. Rabal, “Speckle time evolution characterization by the co-occurrence matrix analysis,” Opt. Laser Technol., vol. 31, no. 2, pp. 163–169, March 1999.

[14] J. H. Vuolo, Fundamentos Da Teoria De Erros, 2nd ed. Blucher, 2019.